Carbon Nanofibers "Spot-Welded" to Carbon Paper by Carbothermal Reduction: A Nano/Micron-Scale Hierarchical Architecture having Low Contact Resistance

Jiang Li,[†] Eve S. Steigerwalt,[‡] Senthil Sambandam,[§] Weijie Lu,[§] and Charles M. Lukehart*,[†]

Department of Chemistry, Vanderbilt University, Nashville, Tennessee 37235, Dana Corporation, Paris, Tennessee 38242, and Departments of Chemistry and Physics, Fisk University, Nashville, Tennessee 37208

Received July 24, 2007. Revised Manuscript Received September 24, 2007

The synthesis, characterization, and electrical measurements of graphitic carbon nanofiber (GCNF)/carbon paper composite materials are reported. GCNF/carbon paper composites having relatively weak GCNF/carbon paper and GCNF/SiO_2/carbon paper interfacial binding are prepared by growing carbon nanofibers directly from growth catalyst nanoparticles distributed throughout the carbon paper support. Carbothermal reduction of GCNF/SiO_2/carbon paper composites effectively "spot welds" carbon nanofibers to carbon paper fibers affording mechanically robust GCNF/SiC/carbon paper composite materials. Characterization methods include scanning electron microscopic imaging, chemical composition and elemental mapping by energy-dispersive X-ray spectroscopy, X-ray diffraction and Raman spectroscopy for phase identification, BET surface-area analysis, and measurement of in-plane and contact electrical resistance. Plots of the pressure dependence of the contact resistance of GCNF/carbon paper and GCNF/SiC/carbon paper composites fall between those of commercial plain carbon paper and wet-proofed carbon paper with the GCNF/SiC/carbon paper composite having a contact resistance similar to that of plain carbon paper. A method for instilling a nano/microscale hierarchical architecture to carbon paper without incurring significant increase of contact resistance is reported.

Introduction

Improving fuel cell technology is of great current interest as energy sustainability and environmental protection become global objectives.[1–4] Of the different types of fuel cells, polymer electrolyte membrane (PEM) fuel cells are being developed for automobile propulsion and as portable power supplies.

Carbon paper is commonly used as the principal structural component of gas diffusion layer (GDL) media contained within PEM fuel cell electrode compartments.[5] Conventional GDL media consist of macroporous/microporous/catalyst trilayer assemblies in which commercially available carbon paper or wet-proofed carbon paper serves as the macroporous layer. A blend of carbon black and poly(tetrafluoroethylene) (PTFE) forms a microporous layer onto which electrocatalyst is deposited, completing typical GDL fabrication. The microporous carbon black component conducts electrons away from catalyst nanoparticles toward the carbon paper and onto a bipolar plate. Within each layer of a PEM fuel cell stack, electrical resistance between bipolar plates, mainly caused by the bulk resistance of GDL media and by GDL/bipolar plate contact resistance, imposes an undesired reduction of fuel cell output voltage up to 25%.[1,5] Hence, there is a critical need to develop novel carbon paper materials that enhance GDL electron flow from catalyst particles yet minimize GDL/bipolar plate contact resistance.[6,7]

We hypothesize that commercial carbon paper containing directly incorporated carbon nanofibers might serve as novel GDL media. Two of the three layers of conventional GDLs could be replaced by a nano/microscale carbon nanofiber/carbon paper hierarchical architecture, where the nanofiber component acts as a high-surface-area catalyst support having high electrical conductivity. While nanocarbon/graphite and nanocarbon/carbon paper composites have been used as electrodes,[8–17] and nanocarbon additives are known to enhance the electrical conductivity of metal/oxide and

* To whom correspondence should be addressed. E-mail: chuck.lukehart@vanderbilt.edu.
[†] Vanderbilt University.
[‡] Dana Corporation.
[§] Fisk University.

(1) Winter, M.; Brodd, R. J. *Chem. Rev.* **2004**, *104*, 4245–4269.
(2) de Bruijn, F. *Green Chem.* **2005**, *7*, 132–150.
(3) Carrette, L.; Friedrich, K. A.; Stimming, U. *Chemphyschem* **2000**, *1*, 162–193.
(4) Lashway, R. W. *MRS Bull.* **2005**, *30*, 581–583.
(5) Blunk, R. H. J.; Lisi, D. J.; Yoo, Y. E.; Tucker, C. L. *AICHE J.* **2003**, *49*, 18–29.
(6) Mishra, V.; Yang, F.; Pitchumani, R. *J. Fuel Cell Sci. Technol.* **2004**, *1*, 2–9.
(7) Williams, M. V.; Begg, E.; Bonville, L.; Kunz, H. R.; Fenton, J. M. *J. Electrochem. Soc.* **2004**, *151*, A1173–A1180.
(8) Steigerwalt, E. S.; Deluga, G. A.; Lukehart, C. M. *J. Phys. Chem. B* **2002**, *106*, 760–766.
(9) Steigerwalt, E. S.; Deluga, G. A.; Lukehart, C. M. *J. Nanosci. Nanotechnol.* **2003**, *3*, 247–251.
(10) He, Z. B.; Chen, J. H.; Liu, D. Y.; Tang, H.; Deng, W.; Kuang, W. F. *Mater. Chem. Phys.* **2004**, *85*, 396–401.
(11) Sun, X.; Li, R.; Villers, D.; Dodelet, J. P.; Desilets, S. *Chem. Phys. Lett.* **2003**, *379*, 99–104.
(12) Wang, C.; Waje, M.; Wang, X.; Tang, J. M.; Haddon, R. C.; Yan, Y. S. *Nano Lett.* **2004**, *4*, 345–348.
(13) Villers, D.; Sun, S. H.; Serventi, A. M.; Dodelet, J. P.; Desilets, S. *J. Phys. Chem. B* **2006**, *110*, 25916–25925.

10.1021/cm701996n CCC: $37.00
Published on Web 11/08/2007

polymer materials,[18,19] the preparation of nanocarbon fiber/carbon paper composites optimized for minimum contact resistance has not been demonstrated.

We now report the synthesis of herringbone graphitic carbon nanofiber (GCNF)/carbon paper, herringbone GCNF/SiO_2/carbon paper, and herringbone GCNF/SiC/carbon paper composite materials as the first effort to optimize both the interfacial binding and the contact resistance within a nanocarbon/microcarbon architecture. GCNF/carbon paper and GCNF/SiO_2/carbon paper composites are prepared by growing GCNFs from either unsupported or silica-supported metal growth catalyst nanocrystals dispersed throughout plain carbon paper. However, subsequent carbothermal reduction of as-prepared GCNF/SiO_2/carbon paper composites initiates the conversion of SiO_2 to SiC giving GCNF/SiC/carbon paper composites, in which GCNF nanofibers are effectively "spot welded" onto the interwoven micron-scale fibers of the carbon paper support. Property measurements of these new materials indicate that GCNF/SiC/carbon paper composites possessing a nanocarbon/microcarbon hierarchical architecture have a contact resistance superior to that of commercial wet-proofed carbon paper and similar to the contact resistance properties of commercial carbon paper.

Experimental Section

General Methods. Two types of carbon paper samples (under the same catalog number TGPH-060), plain carbon paper (sample **1**) and standard wet-proofed carbon paper (sample **2**) were purchased from E-TEK Division, PEMEAS Fuel Cell Technologies and were cut into small sizes (10 mm × 10 mm unless specified) for further use. Scanning electron microscopic (SEM) images were recorded on a Hitachi S-4200 electron microscope using an accelerating voltage at 5 kV, while energy-dispersive X-ray spectra (EDX) and elemental mapping images were obtained with an accelerating voltage of 20 kV. Raman spectra were obtained at room temperature on a LabRam Infinity MicroRaman spectrometer using a He–Ne laser with the excitation line at 632.81 nm through a 100× optical focus microscope. X-ray diffraction (XRD) scans were obtained using a Scintag X_1 θ/θ automated powder X-ray diffractometer with a Cu target, a Peltier-cooled solid-state detector, and a zero-background Si (510) support. Brunauer–Emmett–Teller (BET) surface area (S_{BET}) analysis was determined from N_2 adsorption/desorption isotherms recorded with a Quantachrome NOVA 1000 high-speed surface-area analyzer. In-plane electrical resistivity (ρ) was measured with the van der Pauw technique at room temperature.[20–22] The thickness of the as-received plain carbon paper was measured to be 0.22 mm. Each corner of the square carbon paper samples was connected to a four-probe station (Micromanipulator Company). Electrical current was measured with a Keithley 2410 high-voltage SourceMeter, whereas sample voltage was measured with a Keithley 6514 system electrometer.

Carbon paper was cut into squares of 25.4 mm dimension, and GCNF/carbon paper samples were prepared as described below for contact resistance measurements. The measurements were conducted using an external press to provide controllable pressures.[6] Two carbon paper samples sandwiched one graphite plate with the same 25.4 mm size, forming a measurement assembly placed between two gold plates of the press. Electrical resistance between two gold plates was measured using a Valhalla Scientific 4300B Digital Micro-ohmmeter under a constant current of 10 A. Resistance at each applied pressure was measured three times and the average values were plotted.

Preparation of GCNF/Carbon Paper Composites. *w-GCNF/Carbon Paper Composite*, **3**. Iron–copper catalyst precursor powders with a respective atomic ratio of 7:3 were prepared by coprecipitation of the corresponding metal nitrate solutions with ammonium bicarbonate as reported previously.[23] The precipitate was dried at 110 °C for 18 h and ground into fine powders. The Fe_7Cu_3 catalyst precursor powders (5 mg) were dispersed in 0.5 mL of ethanol using low-power sonication for 5 min and deposited onto a small piece of as-received plain carbon paper substrate. The solvent was evaporated at 110 °C for 18 h, and the dried sample was placed into a tube furnace. Wide herringbone GCNFs (w-GCNFs) with diameters of 100–200 nm were grown on the carbon paper substrate by in situ reducing the catalyst precursor using hydrogen gas and then by catalytically decomposing ethylene at 600 °C for 90 min,[23] affording w-GCNF/carbon paper sample, **3**.

n-GCNF/SiO_2/Carbon Paper Composite, **4**. The Fe_2Ni_8/silica catalyst precursor (3 mg), prepared as reported earlier,[8] was dispersed in 0.5 mL of ethanol using low-power sonication for 5 min. The dispersion was dropped onto a small piece of plain carbon paper and then dried at 110 °C for 18 h. After being transferred into a tube furnace, the catalyst precursor was calcined in air at 400 °C for 4 h, reduced in H_2/He flow (50:200 mL/min) at 350 °C for 20 h, and then heated at 600 °C for 2 h. Narrow herringbone GCNFs (n-GCNFs) having diameters of 15–25 nm were grown on the surface of carbon paper fibers by introducing carbon monoxide at a flow rate of CO/H_2/He = 200:50:50 mL/min at 600 °C for 10 h, yielding n-GCNF/SiO_2/carbon paper sample, **4**.

n-GCNF/SiC/Carbon Paper Composite, **5**. A piece of n-GCNF/SiO_2/carbon paper sample, **4**, was placed into a graphite furnace (Oxy-Gon Industries). The furnace atmosphere was reduced to a pressure of 2.0×10^{-5} Torr and heated at 300 °C for 10 min. Then the furnace was filled with high purity of Ar (99.9999%) and heated to 1650 °C for 30 min. The ensuing carbothermal reduction process yielded n-GCNF/SiC/carbon paper sample, **5**.

Acid-Etched n-GCNF/SiC/Carbon Paper Composite, **6**. A piece of sample **5** was soaked in HCl solution (6.3 mL of ethanol and 28.7 mL of concentrated hydrochloric acid) for 24 h and washed with ethanol/water (volume ratio of 1:1) until washings had a neutral pH value. Then the sample was washed with ethanol and dried under vacuum at room temperature to yield HCl-etched n-GCNF/SiC/carbon paper sample, **6**.

Results and Discussion

Figure 1 shows a schematic representation of the synthesis strategies used to prepare GCNF/carbon paper composites **3**–**5**. SEM images of carbon paper and these materials are shown in Figures 2 and 3. As-received plain carbon paper,

(14) Chen, L. H.; AuBuchon, J. F.; Chen, I. C.; Daraio, C.; Ye, X. R.; Gapin, A.; Jin, S.; Wang, C. M. *Appl. Phys. Lett.* **2006**, *88*, 033103.
(15) Caillard, A.; Charles, C.; Boswell, R.; Brault, P.; Coutanceau, C. *Appl. Phys. Lett.* **2007**, *90*, 223119.
(16) Caillard, A.; Charles, C.; Boswell, R.; Brault, P. *Nanotechnology* **2007**, *18*, 305603.
(17) Barton, S. C.; Sun, Y. H.; Chandra, B.; White, S.; Hone, J. *Electrochem. Solid State Lett.* **2007**, *10*, B96–B100.
(18) Flahaut, E.; Peigney, A.; Laurent, C.; Marliere, C.; Chastel, F.; Rousset, A. *Acta Mater.* **2000**, *48*, 3803–3812.
(19) Dalmas, F.; Dendievel, R.; Chazeau, L.; Cavaille, J. Y.; Gauthier, C. *Acta Mater.* **2006**, *54*, 2923–2931.
(20) van der Pauw, L. J. *Philips Res. Rep.* **1958**, *13*, 1–9.
(21) van der Pauw, L. J. *Philips Tech. Rev.* **1958**, *20*, 220–224.
(22) Kasl, C.; Hoch, M. J. R. *Rev. Sci. Instrum.* **2005**, *76*, 033907.
(23) Li, J.; Vergne, M. J.; Mowles, E. D.; Zhong, W. H.; Hercules, D. M.; Lukehart, C. M. *Carbon* **2005**, *43*, 2883–2893.

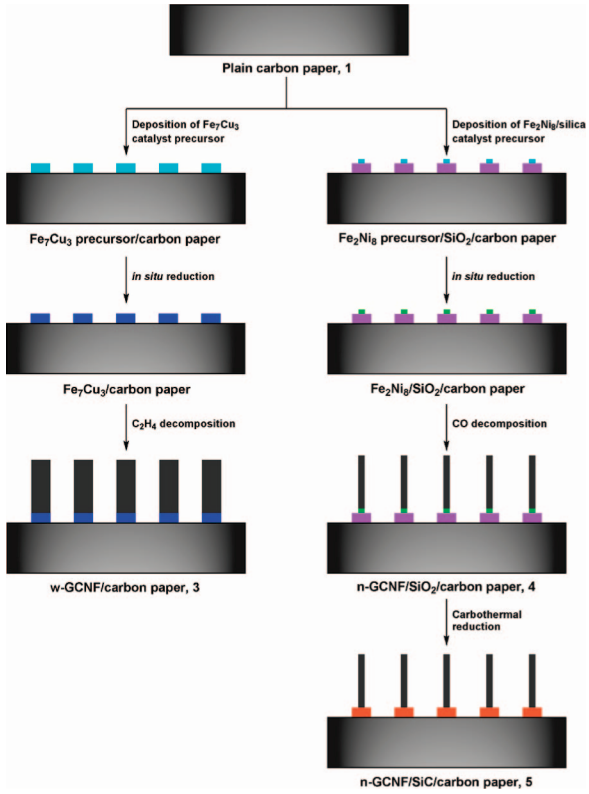

Figure 1. Schematic representation of GCNF/carbon paper composite compositions and synthesis methods.

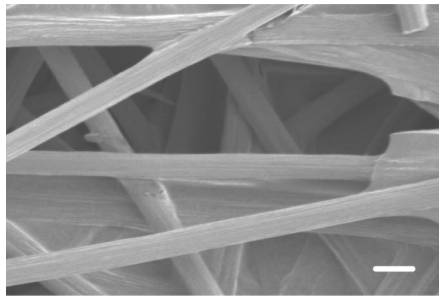

Figure 2. SEM image of as-received plain carbon paper **1**. Scale bar, 10 μm.

1, (see Figure 2), consists of interwoven, straight carbon fibers ca. 6 μm in diameter bound together by unsaturated polyester resins.[24] Mixed-metal carbonate particles dispersed throughout commercial plain carbon paper form metal alloy growth catalyst nanoparticles upon hydrogen reduction. Under appropriate conditions, wide herringbone GCNFs (w-GCNFs) grow from the surfaces of Fe_7Cu_3 growth catalyst nanoparticles dispersed within commercial carbon paper support in the presence of ethylene[18] to give the w-GCNF/carbon paper composite, **3**. These GCNFs have diameters of 100–200 nm (Figure 3a and b) and form a mat-like morphology. Individual nanofibers protrude from the surface of the carbon paper fiber substrate, yet intertwine with other carbon nanofibers. Likewise, narrow herringbone GCNFs (n-GCNFs) grow from the surfaces of much smaller Fe_2Ni_8 growth catalyst nanoparticles supported on flakes of fumed silica and dispersed throughout commercial carbon paper

(24) www.torayca.com (accessed July 2007).

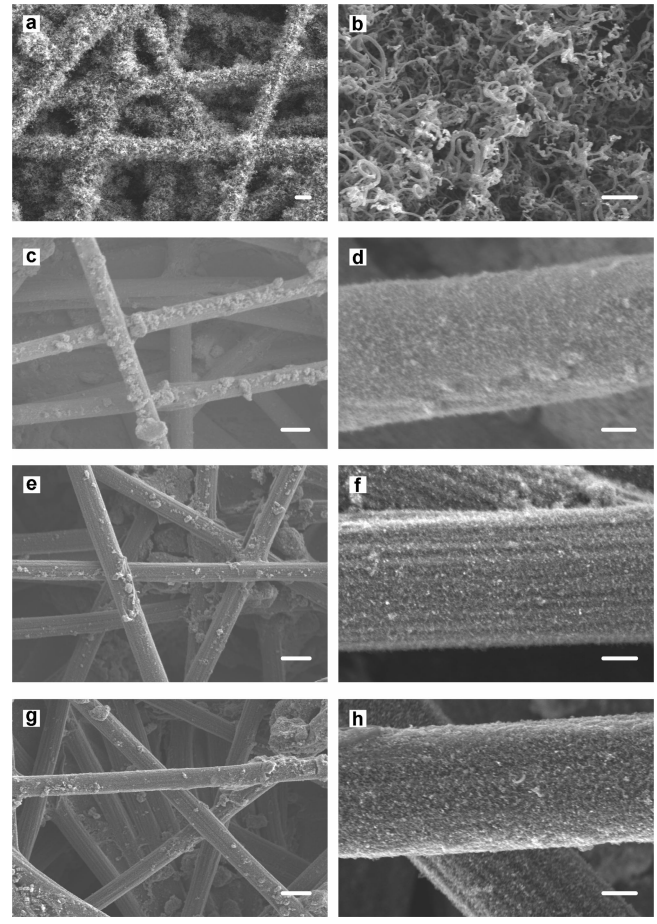

Figure 3. SEM images of (a, b) w-GCNF/carbon paper **3**, (c, d) n-GCNF/SiO_2/carbon paper **4**, (e, f) n-GCNF/SiC/carbon paper **5**, and (g, h) HCl-etched n-GCNF/SiC/carbon paper **6** composites. Scale bars: 10 μm for (a, c, e, g); 2 μm for (b, d, f, h).

support in the presence of CO gas[8] to give the n-GCNF/SiO_2/carbon paper composite, **4**. These GCNFs have diameters of 15–25 nm (Figure 3c and d) and wrap the micron-scale fibers of the carbon paper forming a dense mat less than 1 μm thick. Mild mechanical agitation of composites **3** and **4** leads to noticeable loss of the GCNF component, indicating weak GCNF/carbon paper binding.

Subjecting n-GCNF/SiO_2/carbon paper composite **4** to the conditions appropriate for carbothermal reduction initiates in situ transformation of SiO_2 to SiC at the GCNF/SiO_2 and SiO_2/carbon paper interfaces affording the n-GCNF/SiC/carbon paper composite, **5** (Figure 3e and f). A slightly enhanced vertical protrusion of individual nanofibers is observed. Fortuitously, this carbothermal process effectively "spot welds" the carbon nanofibers to surface sites of the much larger carbon paper fibers giving a mechanically very robust composite. The carbon nanofiber component of composite **5** survives vigorous mechanical agitation. Strong interfacial binding between SiC and carbon nanotube surface sites is known to occur in related SiC growth processes.[25] Subjecting n-GCNF/SiC/carbon paper composite **5** to hydrochloric acid solution etches away any residual metal

(25) Morisada, Y.; Maeda, M.; Shibayanagi, T.; Miyamoto, Y. *J. Am. Ceram. Soc.* **2004**, *87*, 804–808.

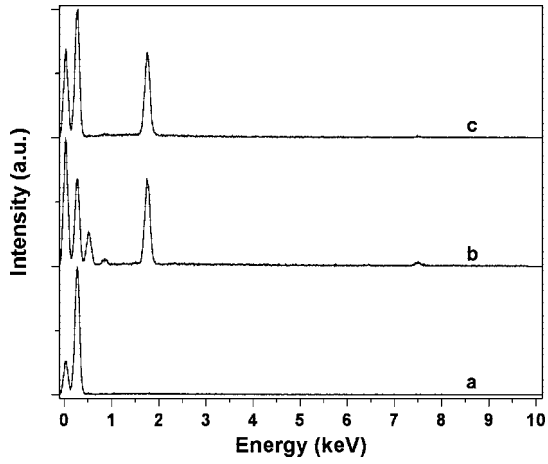

Figure 4. EDX spectra of (a) w-GCNF/carbon paper **3**, (b) n-GCNF/SiO_2/carbon paper **4,** and (c) n-GCNF/SiC/carbon paper **5** composites. Peaks at ca. 0.03 keV are generated from noise emission sources.

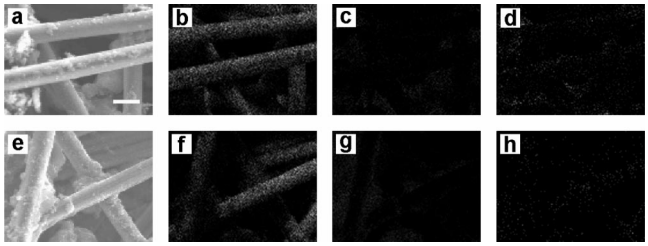

Figure 5. SEM images and elemental mapping patterns of (a–d) n-GCNF/SiO_2/carbon paper **4**, and (e–h) n-GCNF/SiC/carbon paper **5** composites. (a, e) SEM images, (b, f) C maps, (c, g) Si maps, and (d, h) O maps. Scale bar, 10 μm.

growth catalyst giving the n-GCNF/SiC/carbon paper composite **6** with no noticeable change in nanofiber morphology (Figure 3g and h).

EDX spectral data shown in Figure 4 are consistent with the elemental compositions expected for these composites. As-prepared w-GCNF/carbon paper composite **3** (Figure 4a) shows an intense emission peak from carbon (0.27 keV), while emissions from iron and copper growth catalyst particles are absent given the very low abundance of these elements. For n-GCNF/SiO_2/carbon paper composite **4** (Figure 4b), emission peaks expected for carbon, silicon (1.75 keV), and oxygen (0.53 keV) are observed along with weak emission peaks for nickel catalyst (0.85 and 7.49 keV). However, the EDX spectrum of n-GCNF/SiC/carbon paper composite **5** (Figure 4c) reveals emission peaks for only C and Si (along with a very weak peak for residual Ni). Under carbothermal treatment at 1650 °C, conversion of silica to SiC reduces the oxygen content to below detection limits.

Elemental mapping patterns (see Figure 5) of the C, Si, and O contents of GCNF/carbon paper composites **4** and **5** corroborate the above EDX spectral data and provide additional compositional information. The carbon map of the n-GCNF/SiO_2/carbon paper composite **4** (Figure 5b) shows bright spots in a pattern replicating the GCNF/carbon paper SEM image (Figure 5a). The corresponding silicon and oxygen maps (Figure 5c and d) show elemental distributions replicating the GCNF/carbon paper image but at much lower brightness due to the low SiO_2 content within this sample. For the n-GCNF/SiC/carbon paper composite **5**, carbon and

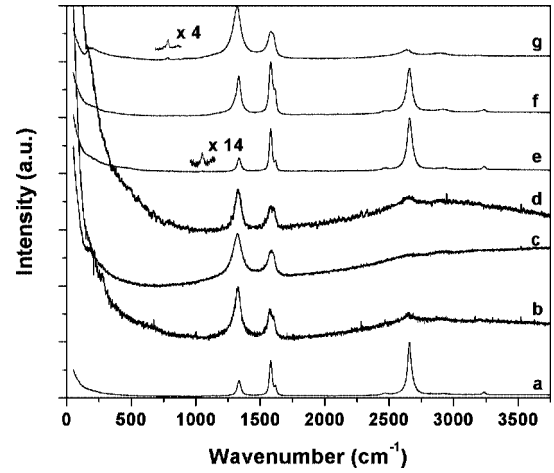

Figure 6. Raman spectra of (a) as-received plain carbon paper **1**, (b) free w-GCNF powders, (c) w-GCNF/carbon paper **3**, (d) free n-GCNF powders, (e) Fe_2Ni_8/silica catalyst precursor supported on carbon paper, (f) n-GCNF/SiO_2/carbon paper **4**, and (g) n-GCNF/SiC/carbon paper **5** composites. Inserts of spectra (e) and (g) show magnified intensity regions.

silicon maps (Figure 5f and g) replicate the GCNF/carbon paper SEM image (Figure 5e); however, the oxygen map (Figure 5h) shows only a very weak pattern consistent with nearly complete carbothermal conversion of SiO_2 to SiC. [Residual SiO_2 support material can be removed completely by either extending carbothermal reaction time or by aqueous HF-etching.] For composites **4** and **5**, the relatively low spot densities observed in the Si elemental maps (and in the oxygen map of composite **4**) are consistent with the presence of SiO_2 and SiC at discrete locations within the samples, consistent with SiC formation at localized sites.

Raman spectra of carbon paper materials **1**, **3–5** and several control samples are shown in Figure 6. Raman bands of as-received plain carbon paper **1** (Figure 6a) at 1320, 1580, 1620, 2660, 2925, and 3240 cm^{-1} are readily assigned to the D-, G-, D′-, 2D-, D+G, and 2D′-bands of graphite, respectively.[26] Large 2D-band/D-band and G-band/D-band intensity ratios are characteristic features of carbon fibers.[27] Raman spectra of free w-GCNF powders (Figure 6b), w-GCNF/carbon paper composite **3** (Figure 6c), free n-GCNF powders (Figure 6d), and n-GCNF/SiO_2/carbon paper composite **4** (Figure 6f) reveal similar graphite scattering peaks. Those samples containing GCNF nanofibers show enhanced relative intensity of the D-band peak due to the high defect content of nanographite materials.[28] The Raman spectrum of a Fe_2Ni_8/silica catalyst *precursor*/carbon paper composite prior to GCNF growth (Figure 6e) has sufficient SiO_2 content to show a weak peak at 1049 cm^{-1} for the Si–O asymmetric stretching vibration of the silica phase.[29] This peak is too weak to be observed in the Raman spectrum of the corresponding n-GCNF/SiO_2/carbon paper composite **4** following GCNF growth. However, carbothermal treatment of composite **4** gives n-GCNF/SiC/carbon paper composite

(26) Endo, M.; Kim, Y. A.; Takeda, T.; Hong, S. H.; Matusita, T.; Hayashi, T.; Dresselhaus, M. S. *Carbon* **2001**, *39*, 2003–2010.
(27) Lespade, P.; Marchand, A.; Couzi, M.; Cruege, F. *Carbon* **1984**, *22*, 375–385.
(28) Pimenta, M. A.; Dresselhaus, G.; Dresselhaus, M. S.; Cancado, L. G.; Jorio, A.; Saito, R. *Phys. Chem. Chem. Phys.* **2007**, *9*, 1276–1291.
(29) Lu, W. J.; Steigerwalt, E. S.; Moore, J. T.; Sullivan, L. M.; Collins, W. E.; Lukehart, C. M. *J. Nanosci. Nanotechnol.* **2004**, *4*, 803–808.

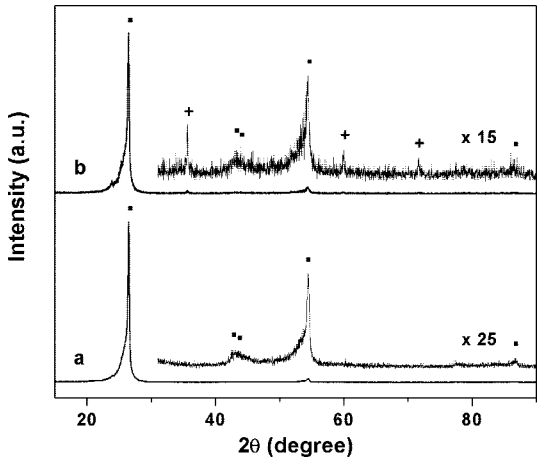

Figure 7. XRD scans of (a) as-received plain carbon paper **1** and (b) n-GCNF/SiC/carbon paper **5** composites. Peaks with (•) come from graphite phase while those indicated by (+) come from silicon carbide phase.

Table 1. Properties of Carbon Paper and GCNF/Carbon Paper Composites

sample no.	sample	S_{BET} (m^2/g)	ρ^a ($\mu\Omega$•m)
1	As-received plain carbon paper	9.2	60.1
2	Standard wet-proofed carbon paper	13.9	73.1
3	w-GCNF/carbon paper	33.9	60.5
4	n-GCNF/SiO_2/carbon paper	–[b]	–[b]
5	n-GCNF/SiC/carbon paper	194.3	69.1
6	HCl-etched n-GCNF/SiC/carbon paper	–[b]	77.0

[a] Standard deviation of 3%. [b] Data not available.

5, and the Raman spectrum (Figure 6g) of composite **5** reveals two weak bands at ca. 195 and 785 cm^{-1}, assigned to the folded transverse acoustic/optical modes of the cubic 3C–SiC phase formed by carbothermal reduction.[30,31]

XRD scans also confirm successful carbothermal transformation of composite **4** to composite **5** (see Figure 7). An XRD scan (Figure 7a) of as-received plain carbon paper **1** shows diffraction peaks at 26.4°, 42.5°, 43.5°, 54.5°, and 86.8° in 2θ assigned, respectively, to the (002), (100), (101), (004), and (006) reflections of graphite (ICDD PDF #41-1487). The relatively high intensity of the (002) peak is consistent with a <002> alignment of carbon paper fibers within the plane of the carbon paper. XRD scans (not shown) of w-GCNF/carbon paper composite **3** and n-GCNF/SiO_2/carbon paper composite **4** are not significantly different from that of as-received plain carbon paper. However, the XRD scan (Figure 7b) of n-GCNF/SiC/carbon paper composite **5** clearly shows the formation of the cubic 3C–SiC phase (ICDD PDF #29-1129) produced by carbothermal reduction. Diffraction peaks at 35.6°, 60.0°, and 71.8° in 2θ are consistent with the (111), (220), and (311) reflections of crystalline 3C–SiC.

BET specific surface areas (S_{BET}) and in-plane electrical resistivities (ρ) of carbon papers and these new GCNF/carbon paper samples are provided in Table 1. The BET specific surface areas of commercial plain carbon paper **1** and wet-proofed carbon paper **2** are 9.2 and 13.9 m^2/g, respectively.

(30) Debernardi, A.; Ulrich, C.; Syassen, K.; Cardona, M. *Phys. Rev. B* **1999**, *59*, 6774–6783.
(31) Nakashima, S.; Kisoda, K.; Gauthier, J. P. *J. Appl. Phys.* **1994**, *75*, 5354–5360.

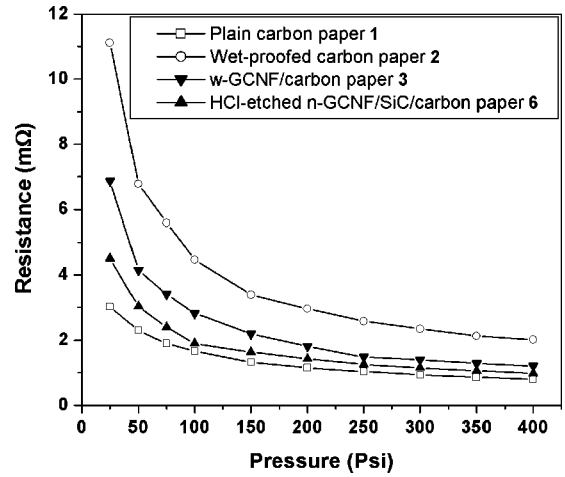

Figure 8. Contact resistance as a function of compression pressure on carbon paper/graphite/carbon paper assemblies, containing as-received plain carbon paper **1**, wet-proofed carbon paper **2**, w-GCNF/carbon paper **3**, or HCl-etched n-GCNF/SiC/carbon paper **6** composites.

However, the BET specific surface area of the w-GCNF/carbon paper composite **3** (33.9 m^2/g) is over three times greater than that of as-received carbon paper due to the presence of a microporous GCNF mat covering the micron-scale fibers of the carbon paper. Similarly, the BET specific surface area of n-GCNF/SiC/carbon paper composite **5** (194.3 m^2/g) is over 20× greater than that of as-received carbon paper due to the presence of a microporous GCNF mat formed by narrower nanofibers of higher surface area. Instilling a nano/microscale GCNF/carbon fiber hierarchical architecture into carbon paper greatly increases specific surface area.

In-plane electrical resistivities (ρ) differ by only 28% (60.1–77.0 $\mu\Omega$•m) among the carbon paper materials tested (see Table 1). As-received plain carbon paper **1** has an in-plane resistivity of 60.1 $\mu\Omega$•m that increases to 73.1 $\mu\Omega$•m for the wet-proofed carbon paper **2** due to the presence of an insulating PTFE coating. The resistivity of w-GCNF/carbon paper composite **3** (60.5 $\mu\Omega$•m) is only slightly greater than that of plain carbon paper (60.1 $\mu\Omega$•m), while a slightly higher resistivity is observed for the n-GCNF/SiC/carbon paper composite **5** (69.1 $\mu\Omega$•m) probably due to the presence of a semiconducting SiC phase at nanocarbon/carbon fiber interfaces. Following HCl washing, the resistivity of composite **6** increases to 77.0 $\mu\Omega$•m, as residual metal growth catalyst has been etched away.

Plots of the total contact resistance of as-received plain carbon paper **1**, wet-proofed carbon paper **2**, w-GCNF/carbon paper composite **3**, and acid-etched n-GCNF/SiC/carbon paper composite **6** as a function of applied pressure are shown in Figure 8. For each sample tested, contact resistance decreases with applied pressure due to pressure-induced enhancement of electrical contact area. Within this set of samples, the contact resistance is lowest for plain carbon paper **1** (3.0 mΩ at 25 psi decreasing to 0.8 mΩ at 400 psi), highest for wet-proofed carbon paper **2** (due to the presence of an insulating PTFE coating), and intermediate for the two GCNF/carbon paper composites **3** and **6**. Of particular importance, total contact resistance of the HCl-etched n-GCNF/SiC/carbon paper composite **6** (4.5 mΩ at 25 psi

to 1.0 mΩ at 400 psi) is nearly equivalent to that of plain carbon paper at applied pressures above 100 psi. It appears that the nano/microscale hierarchical architecture and enhanced mechanical stability of this GCNF/SiC/carbon paper composite compensate for a slightly higher in-plane resistivity to give low contact resistance.

Conclusion

Herringbone graphitic carbon nanofibers having wide (w) or narrow (n) diameters can be grown directly on commercial plain carbon paper using vapor-growth methods to give w-GCNF/carbon paper composites (**3**) and n-GCNF/SiO_2/carbon paper composites (**4**). In situ carbothermal reduction of **4** at 1650 °C transforms the SiO_2 phase to SiC affording a mechanically robust n-GCNF/SiC/carbon paper composite (**5**). SEM images reveal that the GCNF components of these new materials form nanofiber mats covering the surfaces of the micron-scale fibers present within carbon paper. The in-plane resistivities of GCNF-modified carbon paper materials fall between the resistivities of plain and wet-proofed carbon papers. Likewise, the contact resistances of GCNF/carbon papers fall between those of plain and wet-proofed carbon paper with the contact resistance of a HCl-etched n-GCNF/SiC/carbon paper composite being nearly equivalent to that of plain carbon paper at pressures above 100 psi. These results demonstrate that formation of a carbon paper having a nano/micron-scale carbon nanofiber/carbon fiber hierarchical structure and low contact resistance can be achieved using a carbothermal nanofiber/fiber spot-welding synthesis strategy. Further investigation of GCNF/SiC/carbon paper composites as potentially novel GDL media is underway.

Acknowledgment. Financial support through the National Science Foundation Nanoscale Interdisciplinary Research Team Grant CTS-0210366 is gratefully acknowledged.

CM701996N